Published in final edited form as:
J Cell Sci. 2014 March 1; 127(0 5): 1052–1064. doi:10.1242/jcs.141226.

Podosomes of dendritic cells facilitate antigen sampling

Maksim Baranov[#1], **Martin ter Beest**[#1], **Inge Reinieren-Beeren**[1], **Alessandra Cambi**[1], **Carl G. Figdor**[1], and **Geert van den Bogaart**[1]

[1]Department of Tumor Immunology Radboud University Medical Centre Radboud Centre for Molecular Life Sciences Geert Grooteplein 28 6525GA Nijmegen The Netherlands

[#] These authors contributed equally to this work.

Summary

Dendritic cells sample the environment for antigens and play an important role in establishing the link between innate and acquired immunity. Dendritic cells contain mechanosensitive adhesive structures called podosomes that consist of an actin-rich core surrounded by integrins, adaptor proteins and actin network filaments. They facilitate cell migration via localized degradation of extracellular matrix. Here we show that podosomes of human dendritic cells locate to spots of low physical resistance in the substrate (soft spots) where they can evolve into protrusive structures. Pathogen recognition receptors locate to these protrusive structures where they can trigger localized antigen uptake, processing and presentation to activate T-cells. Our data demonstrate a novel role in antigen sampling for podosomes of dendritic cells.

Keywords

Antigen presentation; podosomes; dendritic cells; receptor mediated endocytosis

Introduction

The main function of dendritic cells is antigen presentation. Immature dendritic cells are localized in the spleen and other non-lymphoid tissues and constantly sample tissue and blood for antigens by so-called pattern recognition receptors (PRRs) (Lipscomb and Masten, 2002; McGreal et al., 2005; Takeda and Akira 2005; Kaparakis et al., 2007). Dendritic cells express many different PRRs that recognize pathogen-associated molecular patterns (PAMPs) such as lipopolysaccharide from the outer membrane of gram-negative bacteria as well as peptides of bacterial, fungal or viral origin. Binding of antigen to some PRRs such as C-type lectins can trigger uptake of antigen via receptor-mediated endocytosis or phagocytosis. Recognition of antigen results in maturation of dendritic cells and surface presentation of the antigen by major histocompatibility complex (MHC) molecules, upregulation of specific co-stimulatory molecules and finally migration to the lymph nodes where dendritic cells prime T-cells (Banchereau and Steinman, 1998; McGreal et al., 2005). Because only dendritic cells can induce a primary immune response in resting naive T-

Address correspondence to: Geert van den Bogaart; mail@bogeert.com.

Europe PMC Funders Author Manuscripts

lymphocytes, they are considered a crucial component balancing the innate and adaptive immune systems. For antigen sampling immature dendritic cells need to migrate from their sites of origin (i.e. bone marrow) to specific sites of sampling activity (peripheral tissues) and for activation of T-cells mature dendritic cells need to travel to the draining lymph nodes where they present antigen to T-cells.

Immature dendritic cells form particular cell-matrix contacts called podosomes that facilitate cell migration within peripheral tissues (reviewed in: Buccione et al., 2004; Gimona et al., 2008; Linder et al., 2011; Murphy and Courtneidge, 2011; Schachtner et al., 2013b). Podosomes consist of an actin-rich core region surrounded by integrins from which anti-parallel actin filaments radiate (Schmidt et al., 2011; van den Dries et al., 2013b). Adaptor proteins such as vinculin, talin and paxillin connect the cortical actin cytoskeleton to the plasma membrane and to integrins and are enriched around the actin-rich cores of podosomes. Unlike focal adhesions, podosomes contain the protein WASP that can recruit the Arp2/3-actin nucleating complex (Linder et al., 1999; Burns et al., 2001; Jones et al., 2002; Calle et al., 2006). Podosomes are points of concentrated release of the metalloprotease MMP-14 (also called MT1-MMP) and several other proteases that locally degrade the extracellular matrix (ECM) (van Helden et al., 2006; Gimona et al., 2008; Linder et al., 2011; Murphy and Courtneidge, 2011). Protease release at podosomes promotes cell invasiveness and facilitates cell migration through endothelium, epithelium and connective tissue (Matías-Román et al., 2005; Carman et al., 2007; Linder, 2007; Schachtner et al., 2013b). In fact, podosomes are commonly located at the leading edge of migrating cells and their turnover is required for cell migration and passage through endothelium (Burns et al., 2001; Calle et al., 2006). WASP deficient leukocytes do not form podosomes and chemotactic migration is severely compromised in these cells (Zicha et al., 1998; Jones et al., 2002; Dovas et al., 2009). Podosomes are mechanosensitive (Collin et al., 2008) as demonstrated by their selective localization on the edges of 3D-micropatterned substrates (van den Dries et al., 2012).

Podosomes are not only formed by dendritic cells (Burns et al., 2001) but also by many other types of adherent cells such as smooth muscle cells, endothelial cells, megakaryocytes, fibroblasts, macrophages, osteoclasts, microglia and at the postsynaptic site of the neuromuscular junction (Buccione et al., 2004; van Helden et al., 2006; Proszynski et al., 2009; Linder et al., 2011; Schachtner et al., 2013a). Although podosomes are very similar to the well-studied invadopodia of cancer cells (Wolf and Friedl, 2009) which are involved in cancer metastasis (Sabeh et al., 2004; Bravo-Cordero et al., 2012), they are considered to differ from invadopodia in at least two ways. First, podosomes are very dynamic with lifetimes that can be as short as 1 to 12 minutes, whereas invadopodia can persist for hours (reviewed in: Linder et al., 2011; Murphy and Courtneidge, 2011). Second, podosomes are smaller and measure only 0.5 to 2 μm in diameter and protrude only about 0.4 to 2 μm, whereas invadopodia can reach 8 μm in diameter and can protrude more than 5 μm from the cell surface into the extracellular environment (Linder et al., 2011; Murphy and Courtneidge, 2011). However, the latter is ambiguous and it was recently shown that podosomes of dendritic cells could protrude more than 3 μm into the pores of polycarbonate filters (Gawden-Bone et al., 2010). Thus, the geometry of the substrate not only dictates the

localization of podosomes (van den Dries et al., 2012), but may also affect the morphology of podosomes and allow podosomal protrusion into the extracellular environment.

In the study by Gawden-Bone et al. (2010) it was demonstrated that when dendritic cells were cultured on filters, podosomes formed precisely on top of the pores and could extent into the lumen of the filter pores. Both release of MMP-14 containing vesicles and uptake of extracellular material occurred at the tips of these protrusive structures (Gawden-Bone et al., 2010). These results are interesting because dendritic cells are well known to be capable to sample for antigen in the lumen of the lung, gut and small intestine by extending 'protrusive dendrites' through the epithelium of these organs (Rescigno et al., 2001; Niess et al., 2005; Chieppa et al., 2006; Vallon-Eberhard et al., 2006; Lelouard et al., 2012; Thornton et al., 2012; Farache et al., 2013; Shan et al., 2013; Strisciuglio et al., 2013). We speculated that this trans-epithelial antigen sampling might be related to the protrusive podosome-like structures first described by Gawden-Bone et al. (2010) and performed a molecular characterization of these actin-rich structures. In this study, we demonstrate that podosomes of human dendritic cells can evolve in protrusive structures that help the cell to sample for antigen from well within the substrate. A wide range of PRRs locate to these protrusive structures where they can trigger receptor-mediated uptake of antigen. Our results show a direct role of podosomes in antigen presentation and this constitutes a new mechanism of how cells may be able to sense extracellular signals through physical barriers.

Results

Podosomes extent in soft spots of the substrate

When human dendritic cells are cultured on glass substrate, they form clusters of podosomes (Fig. 1A) (Burns et al., 2001; van Helden et al., 2006). Podosomes on glass appear as dome-shaped actin-rich structures with an actin core of about 350 nm diameter and a height of about 500 nm, surrounded by a 250 nm wide ring of integrins and integrin-associated proteins such as vinculin, talin and paxillin (Labernadie et al., 2010; Schmidt et al., 2011; Cox et al., 2011; van den Dries et al., 2012; van den Dries et al., 2013b). It has been recently reported that when dendritic cells are cultured on polycarbonate filters with pores of defined size, podosomes locate on top of the filter pores (Gawden-Bone et al., 2010). This alignment of the podosomes with the filter pores is likely related to the mechanosensitivity of podosomes that form around local deformations of the substrate (van den Dries et al., 2012). Indeed, when we cultured human dendritic cells for one hour on gelatin-soaked polycarbonate filters with 400 nm diameter pores, almost all podosomes formed directly on top of the filter pores (Fig. 1B–E). The actin-rich cores of these podosomes were surrounded by adaptor proteins such as talin, vinculin and paxillin, similar to podosomes formed by cells on glass substrates (Linder et al., 2011). Optical z-sectioning by confocal microscopy revealed that these podosomes did not protrude into the lumen of the 400 nm-sized pores of the polycarbonate filters (less than 1 μm protrusion depth; Fig. 1B).

We speculated that a pore size of 400 nm might be too small to allow for protrusion of podosomes. To address this, we cultured dendritic cells on gelatin-impregnated filters with larger pores of 1 μm diameter, identical to those employed by Gawden-Bone et al. (2010). Indeed, as reported (Gawden-Bone et al., 2010), we observed clear protrusion of actin-rich

structures into these 1 μm-sized pores (Fig. 2A) and regardless of whether the filters were impregnated with gelatin. The actin-rich core of these podosome-like structures could penetrate through the entire filter of about 10 μm thickness. The actin-rich cores were surrounded by adaptor proteins such as vinculin which was predominantly present at the base of the pores and did not seem to protrude into the 1 μm-sized pores. However, vinculin increasingly protruded into the lumen of the pores when cells were cultured on filters with larger pore sizes of 2 μm and 3 μm in diameter (Fig. 2B–C). On filters with these larger pore sizes, podosomes not exclusively colocalized with the pores but were increasingly also present in between the pores (Fig. 2D). On filters with 3 μm-sized pores, small individual podosomes could be distinguished at the edges of the pores and the pore size was large enough to facilitate migration of the whole cell through the filter pores (Fig. 2C, 2E), as reported previously (Gawden-Bone et al., 2010). Thus, for cells cultured on polycarbonate filters with increasing pore sizes from 400 nm to 3 μm, the morphology of the podosomes differs and first the actin core and later adaptor proteins such as vinculin can progressively protrude into the lumen of the pores.

Overall, a picture is emerging where initial non-protrusive podosomes of dendritic cells search for soft spots of low physical resistance in the substrate (e.g. the filter pores). When such a place is found, podosomes become increasingly invasive and can protrude into the substrate by local degradation of extracellular matrix and by exerting mechanical forces (Gawden-Bone et al., 2010; Labernadie et al., 2010). This results in growth of a protrusive podosome-like structure and at some point (i.e. for pores above 3 μm in diameter; Gawden-Bone et al., 2010) facilitates transmigration of the cell through physical barriers. Dendritic cells and other blood leukocytes have to cross blood vessel and lymphatic endothelium in order to activate the immune system (Muller, 2011; Vestweber, 2012). Secretion of the metalloprotease MMP-14 and turnover of podosomes are well-known to be essential for this transendothelium migration (Matías-Román et al., 2005; Calle et al., 2006; Carman et al., 2007). Indeed, dendritic cells can migrate through monolayers formed by the endothelial cell line EA.hy926 (Supp. Fig. 1A–B). Dendritic cells are also able to penetrate and pass monolayers formed by the epithelial cell line Caco-2 (Supp. Fig. 1C–E) (Rescigno et al., 2001; Strisciuglio et al., 2013) and for megakaryocytes podosomes have recently been shown to play a role in this epithelial penetration as well (Schachtner et al., 2013a). Thus, it is increasingly clear that podosomes facilitate cell migration across both endothelial and epithelial barriers.

Characterization of protrusive podosome-like structures

To closer investigate the protrusive podosome-like structures on filter substrates, we performed immunostainings for typical podosomal marker proteins on dendritic cells cultured on filters with 1 μm pore sizes. Similar to podosomes of cells cultured on glass (Fig. 1A), the F-actin-rich core of protrusive podosome-like structures was surrounded by rings or clusters of talin, paxillin and the integrins ITGAM (subunit of integrin αMβ2) and ITGB1 (integrin β1) (Fig. 3A). Interestingly, protrusive podosome-like structures often (but not always; ~10 – 30% of podosomes) contained a ring of actin at the base of the protrusions as observed with both phalloidin in fixed cells (Fig. 3B) and with the F-actin binding probe LifeAct-GFP in live cells (Supp. Fig. 2A–B). This is in clear contrast to podosomes formed

by cells on glass substrate which are generally considered to contain solid cores of actin (Fig. 1A). Integrins stimulate the production of phosphatidylinositol 4,5-bisphosphate (PIP_2) which stimulates WASP activity (Prehoda et al., 2000) and binds directly to talin and vinculin (Brakebusch and Fässler, 2003) and PIP_2 accumulates at and is essential for the formation of invadopodia of cancer cells (Yamaguchi et al., 2010). We therefore probed for PIP_2 using exogenously added bacterially expressed pleckstrin homology domain of phospholipase C delta subunit fused to citrine (PLCδ-PH) (van den Bogaart et al., 2011). PLCδ-PH stained a ring surrounding the actin-rich core, demonstrating the presence of PIP_2 in this region (Fig. 3C). Podosome-like protrusive structures still depended on WASP (Linder et al., 1999; Burns et al., 2001; Jones et al., 2002; Calle et al., 2006), as treatment of the cells with wiskostatin, a selective and reversible inhibitor of WASP (Peterson et al., 2004), resulted in disassembly of the actin-rich protrusions at a similar rate as podosomes of cells cultured on glass (Fig. 3D–E) (Dovas et al., 2009; Thujita et al., 2013).

Degradation of extracellular matrix occurs at podosomes and is dependent on the local release of metalloproteases such as MMP-14 (Buccione et al., 2004; Gimona et al., 2008; Linder et al., 2011; Schachtner et al., 2013b). Indeed, degradation of extracellular matrix took place at protrusive podosome-like structures as apparent by the (~2-fold) local increased fluorescence intensity when the filters were impregnated with double-quenched FITC-labeled collagen in gelatin (Fig. 4A–B) and in agreement with previous results (Gawden-Bone et al., 2010). We observed by immunocytochemistry that MMP-14 was present in the protrusive podosome-like structures (formed on 1 μm-sized pores) and this is a clear difference from the (nonprotrusive) podosomes of cells cultured on glass where MMP-14 was not enriched but rather seemed excluded from the actin-rich podosome cores (Wiesner et al., 2010) (Fig. 4C). MMP-14 containing vesicles are known to traffic intracellularly by kinesin over microtubules (Wiesner et al., 2010; Cornfine et al., 2011) and to travel via microtubules to the tip of invadopodia of cancer cells (Schoumacher et al., 2010). Our data suggest that MMP-14 containing vesicles could traffic via microtubules to the tip of protrusive podosome-like structures as well, because microtubules clearly penetrated the F-actin ring of these structures and extended into the lumen of the filter pores (Fig. 4D). This tubulin protrusion again contrasts podosomes of cells cultured on glass where the extension of the tubules into the podosomal cores was not observed.

The substrate influences the lifetime of podosomes and periodic undulations of the actin-rich core are proposed to contribute to the protrusive and mechanosensitive properties of podosomes (Schachtner et al., 2013a; van den Dries et al., 2013a). Indeed, podosomes seem to become less dynamic and more stable when they become more invasive, because protrusive podosome-like structures had lifetimes that exceeded several hours compared to less than 1 h for podosomes on glass substrate. Moreover, the periodic undulations of the actin cores of protrusive podosome-like structures were about 2-fold reduced compared to podosomes of cells cultured on glass (Supp. Fig. 2C–E; Supp. Movie 1–2) (see also: Labernadie et al., 2010; van den Dries et al., 2013a). Together, we conclude that when podosomes encounter spots of low physical resistance of the substrate (e.g. the filter pores), their morphology and protein composition change as they become increasingly more protrusive and less dynamic. We then addressed the role of endocytosis at these protrusive podosome-like structures of dendritic cells.

Europe PMC Funders Author Manuscripts

Protrusive podosome-like structures are involved in antigen sampling

In a previous study (Gawden-Bone et al., 2010), uptake of extracellular material at protrusive podosome-like structures of dendritic cells was shown by electron microscopy. In accordance with this observation, we found the coat protein clathrin to localize to these protrusive structures (Fig. 5A–C). Since it is well-established that dendritic cells can sample for antigen across epithelial membranes (Rescigno et al., 2001; Niess et al., 2005; Chieppa et al., 2006; Vallon-Eberhard et al., 2006; Lelouard et al., 2012; Thornton et al., 2012; Farache et al., 2013; Shan et al., 2013; Strisciuglio et al., 2013) and confirmed by our observations with monolayers of the epithelial cell line Caco-2 (Supp. Fig. 1E), we hypothesized that antigen recognition and uptake might occur at the protrusive podosome-derived structures. In order to test this possibility, we first determined whether PRRs involved in antigen uptake located to these protrusive structures. We cultured monocyte derived dendritic cells on filters with 1 μm pore sizes for 1 hour and performed immunostaining for various PRRs: the C-type lectin family receptors DC-SIGN, DCIR, Dectin-1 and the mannose receptor CD206. We also stained for the transferrin receptor CD71 as a general endocytic receptor. All of these PRRs and CD71 localized to protrusive podosome-like structures, but not to non-protrusive podosomes on glass substrates (Fig. 5D–F). The presence of DC-SIGN and CD206 at these protrusive structures was confirmed by immuno-gold labeling followed by transmission electron microscopy (similar to Gawden-Bone et al., 2010), where we observed a ~3-fold (DC-SIGN) to ~9-fold (CD206) enrichment of gold beads at the protrusive structures compared to the ventral membrane of the cells (i.e. membrane in contact with the filter surface) (Fig. 6). We subsequently determined the antigen sampling activity of these PRRs that localize to protrusive podosome-like structures.

We performed functional uptake experiments of quantum dots tethered to gp120 as a prototype antigen (Cambi et al., 2007). The HIV-1 envelope glycoprotein gp120 is a ligand for DC-SIGN (Geijtenbeek et al., 2000) and these gp120-coated quantum dots have a particle size of about 40 nm, comparable to the size of many viruses (Cambi et al., 2007). We also performed uptake experiments with ovalbumin (OVA), a well-characterized antigen and ligand for the mannose receptor CD206 (Burgdorf et al., 2006). Leakage experiments demonstrated that gelatin-impregnated filters were not or only poorly permeable to both OVA and gp120-quantum dots (Fig. 7A–C). We measured cellular uptake of gp120-quantum dots and of OVA through these gelatin-impregnated filters by fluorescence microscopy (Fig. 7D–F). Live cell imaging showed that uptake of OVA through the filter occurred at the actin-rich protrusive structures (Fig. 7F). Uptake could be suppressed by the inhibitor of both clathrin-dependent (von Kleist et al., 2011) and independent (Dutta et al., 2012) endocytosis Pitstop 2, indicating that uptake occurred via endocytosis (Fig. 7G).

Importantly, uptake of both gp120-quantum dots and OVA through the filters was promoted by the presence of protrusive podosome-like structures, because uptake was strongly reduced (i) when the dendritic cells were cultured on filters with 400 nm pore size (where podosomes form but cannot protrude; Fig. 1B) (Fig. 8A–B) and (ii) when CHO cells heterogeneously expressing recombinant DC-SIGN were used instead of dendritic cells (Fig. 8A). These CHO–DC-SIGN cells can take up gp120-quantum dots from the growth medium (Cambi et al., 2007), but do not form podosomes or podosome-like protrusions (Supp. Fig.

3A). (iii) Moreover, uptake of OVA could be inhibited by the WASP inhibitor wiskostatin (Fig. 8C) that results in disassembly of the protrusive structures (Fig. 3D–E). Although the rate of antigen uptake was decreased, uptake was not completely blocked at these control conditions, because of residual leakage of antigen through the filters and because the cells were still able to degrade gelatin. Uptake of gp120-quantum dots and OVA was antigen specific, because (i) uptake could be blocked by competitive inhibition with the sugar mannan (which binds to DC-SIGN and CD206) and (ii) biotin treated quantum dots (i.e. without gp120) were endocytosed substantially less effectively than gp120-quantum dots (Fig. 8A–B).

The antigen was not only taken up by the dendritic cells through the filters, but also subsequently processed by proteases as apparent from the increase in fluorescence of double-quenched OVA (Fig. 8D–E). Degradation of this double-quenched OVA by proteases in endosomal/lysosomal compartments results in loss of fluorescent quenching and an increased fluorescence intensity. Control experiments with bafilomycin demonstrated that this processing was dependent on the acidification of endosomal/lysosomal compartments. Bafilomycin blocks the vesicular ATPase and thereby prevents the acidification required for activation of proteases. We performed experiments with dendritic cells isolated from mouse bone marrow (BMDCs) to determine if dendritic cells that took up OVA antigen via podosomes could activate T-cells. Similar to human dendritic cells, these mouse BMDCs were able to form protrusive podosome-like structures on filters with 1 μm pore sizes and these protrusive structures contained vinculin, metalloprotease MMP-14 and CD206 (the receptor for OVA antigen (Burgdorf et al., 2006)) (Supp. Fig. 3B). Finally, BMDCs that were loaded with OVA antigen via the filters could activate mouse hybridoma DO11.10 T-cells (Supp. Fig. 3C). DO11.10 T-cells recognize ovalbumin (323–339 epitope) bound to MHC class II and this results in an increased secretion of IL-2 (Shimonkevitz et al., 1983). However, due to (i) the great sensitivity of T-cells, (ii) the limited amount of dendritic cells we could culture on the filters (~10^3 cells) and (iii) the inability to completely wash OVA from the gelatin coated filters (due to non-specific binding), we were unable to exclude the possibilities that antigen was directly taken up from the medium during the prolonged T-cell incubation step or that antigen leaked out of the cells or was regurgitated to be presented to the T-cells in *trans* rather than in *cis*. Nevertheless, co-localization experiments indicated that the antigen at least partly reached MHC class II containing compartments in human dendritic cells (Fig. 8F). We conclude that antigen uptake can occur at protrusive structures of dendritic cells that contain podosomal elements and this antigen can be subsequently processed by dendritic cells which might eventually result in T-cell activation.

Discussion

In this study we demonstrate that podosomes can evolve into protrusive structures that can contribute to antigen sampling of dendritic cells. It is increasingly well established that podosomes respond to and sense the stiffness and geometry of the cellular substrate (Collin et al., 2008; Labernadie et al., 2010; van den Dries et al., 2012). Podosomes localize to spots of low physical resistance in the substrate. At these soft spots, podosomes exert physical forces (Labernadie et al., 2010) and locally degrade extracellular matrix by the concentrated release of metalloproteases such as MMP-14 (Buccione et al., 2004; Gimona et al., 2008;

West et al., 2008; Gawden-Bone et al., 2010; Linder et al., 2011; Schachtner et al., 2013b). This can result in remodeling of the extracellular matrix and when or if pores are formed of sufficiently large size (> 1 μm), podosomes become progressively protrusive and less dynamic and the morphology and protein composition of podosomes change. These findings are in agreement with the role of invasive podosome-like structures in the formation of transcellular pores in endothelium (Carman et al., 2007).

At least at the base of protrusive podosome-like structures, actin forms a ring-shaped structure that aligns with the edges of the pore. This contrasts (non-protrusive) podosomes on glass substrates which are generally considered to consist of solid cores of actin, although recent STORM super-resolution microscopy data from our group seems to suggest also in this case an uneven distribution of actin in podosome cores that cannot be resolved by conventional diffraction limited microscopy (van den Dries et al., 2013b). Microtubules penetrate the actin ring of the protrusive podosome-like structures and likely facilitate delivery of MMP-14 containing vesicles to the protrusive tips (Wiesner et al., 2010; Cornfine et al., 2011), similar to invadopodia of cancer cells where this is well established (Schoumacher et al., 2010). This again contrasts podosomes on glass substrates where MMP-14-containing vesicles do not seem to reach the core but only transiently contact the periphery of podosomes (Wiesner et al., 2010) and here perhaps the dense actin cores prevent the entry of microtubules.

Eventually, the combined effects of the mechanical forces exerted by the podosomes and the protease-mediated degradation of extracellular material can allow for the complete cell to migrate through physical barriers. Here, pores in the substrate need to exceed a threshold size (~ 3 μm) (Gawden-Bone et al., 2010) which is likely limited by the size of the nucleus (Wolf et al., 2013). Migration of dendritic cells and other leukocytes through extracellular matrix and across endothelial membranes of blood and lymph vessels is critical for immune system function (Muller, 2011; Vestweber, 2012) and our data further support the well-established role of podosomes in this process (Zicha et al., 1998; Burns et al., 2001; Jones et al., 2002; Matías-Román et al., 2005; Calle et al., 2006; Dovas et al., 2009).

In our study we demonstrate a clear role of podosomes in antigen sampling of dendritic cells. We showed that when podosomes become progressively protrusive, a variety of PRRs localize to these protrusive structures. These PRRs allow for receptor-mediated uptake of antigen from the protrusive tips (Gawden-Bone et al., 2010) and thereby can help the cell to sample for antigens from well within the substrate (i.e. from the other side of the polycarbonate filter). Antigen can not only be taken up, but can also be subsequently processed and trafficked to MHC class II compartments and after antigen presentation this may result in T-cell activation. Interestingly, it was recently reported that T-cells also employ protrusive podosome-like structures that contain T-cell receptors to probe for peptide presentation in MHC class I and II (Sage et al., 2012), in clear analogy to our findings of antigen recognition by podosomes of dendritic cells.

A body of evidence suggests that dendritic cells can sample for antigen across lung, gut and small intestine epithelium (Rescigno et al., 2001; Niess et al., 2005; Chieppa et al., 2006; Vallon-Eberhard et al., 2006; Lelouard et al., 2012; Thornton et al., 2012; Farache et al.,

2013; Shan et al., 2013; Strisciuglio et al., 2013). Here, dendritic cells can extent protrusive dendrites across the tight junctions of epithelial cells (Rescigno et al., 2001) or through transcellular pores in specialized microfold (M) cells (Lelouard et al., 2012) and this facilitates the uptake of bacteria from the apical (lumen) side of the epithelial membrane. Our findings now suggest that these protrusive transepithelial dendrites may have evolved from podosomes and thus could provide a mechanistic explanation for the capability of dendritic cells to phagocytose intraepithelial bacteria.

In summary, we showed that podosomes can sample the extracellular environment for spots of low mechanical resistance and once such a spot is identified podosomes can become increasingly protrusive. These protrusive structures not only facilitate cellular migration through extracellular matrix and endothelial membranes, but can also be engaged in receptor-mediated uptake of antigen. Thereby podosomes can effectively increase the search area that a dendritic cell samples for antigen. This localized uptake of antigen from podosome-derived protrusive structures constitutes a novel role for podosomes of dendritic cells. Understanding how dendritic cells and other monocytes sample for antigen in the complex physical environment of the human body is crucial for our understanding of immune function.

Materials and Methods

Preparation of human dendritic cells

Dendritic cells were derived from peripheral blood monocytes isolated from a buffy coat (de Vries et al., 2002). Monocytes isolated from healthy blood donors were cultured for 6 days in RPMI 1640 medium (Life Technologies) containing 10% fetal bovine serum (FBS, Greiner Bio-one), 1 mM ultra-glutamine (BioWhittaker), antibiotics (100 U ml^{-1} penicillin, 100 μg ml^{-1} streptomycin and 0.25 μg ml^{-1} amphotericin B, Gibco), IL-4 (500 U ml^{-1}) and GM-CSF (800 U ml^{-1}) in a humidified, 5% CO_2-containing atmosphere.

Antibodies and reagents

The following primary antibodies were used for the immunofluorescence: mouse anti-vinculin (V9131, Sigma) at 1:200 dilution (v/v), mouse anti-talin (T3287, Sigma) at 1:100 (v/v), mouse anti-paxillin (349 | MAB3060, Sigma) at 1:100 (v/v), mouse anti-CD11b (ITGAM or Bear-1) (IM2581, Coulter) at 1:200 (v/v), mouse anti-CD29 (or ITGB1) (clone ts2/16) at 1:200 (v/v), mouse anti-MMP-14 (MAB3328, Bio Connect / MilliPore) at 1:100 (v/v), rat anti-tubulin (ab6161, Abcam) at 1:500 (v/v), mouse anti-human CD209 (or DC-SIGN) (551186, BD Bioscience) at 1:200 (v/v), mouse anti-human DCIR (DDX0180, Dendritics) at 1:200 (v/v), mouse anti-human Dectin-1 (MAB1859, R&D Systems) at 1:100 (v/v), mouse anti-human CD206 (555953, BD Biosciences) at 1:250 (v/v), mouse anti-human CD71 (347510, SALK) at 1:50 (v/v), mouse anti-clathrin light chain (C1985, Sigma) at 1:100 (v/v) and mouse anti-human MHC class II (clone Q5/13 (Quaranta et al., 1980)) at 20 μg ml^{-1}. The following secondary antibodies were used: goat anti-mouse IgG (H+L) (A-11001), goat anti-rat IgG (H+L) (A-11006) and goat anti-rabbit IgG (H+L) (A-11008), all labeled with Alexa fluor 488 dye (Invitrogen). Alexa fluor 488, 546 and 633 conjugated phalloidin (Invitrogen) was used at dilutions of 1:200 (v/v) to stain F-actin. Qdot

Streptavidin Conjugate 655 nm was from Invitrogen (Q10121MP). Biotin rgp120 (HIV-1 III B) was purchased from ImmunoDiagnostics.

Gelatin impregnated filters

Gelatin was labeled with Alexa fluor 633 by incubating 2% (w/v) gelatin from porcine skin in PBS with 100 μg ml^{-1} Alexa fluor 633 succinimidyl ester (Invitrogen) for 30 min at room temperature. Unbound dye was removed by methanol precipitation of the gelatin. Hydrophilic polycarbonate membrane filters with different pore sizes (0.4, 1, 2, 3 μm; 13 mm in diameter) (PCT0413100, PCT1025100, PCT2013100, PCT3013100; all from Sterlitech, Kent, WA) were washed first in 70% and then in 96% ethanol at room temperature. A 5 μl droplet of 2.5% gelatin in PBS was placed on top of a parafilm sheet (sterilized with ethanol) and a filter together with a cover slip was positioned on top of the gelatin solution. After 10 min of incubation the filters were detached from the cover slips and subsequently transferred into a 24 well plate and kept in PBS until needed for cell culturing.

DQ-FITC conjugated collagen (Invitrogen) was used for detection of extracellular matrix degradation. Human immature dendritic cells were grown for 1 hour on filters prepared with 2.5 μg ml^{-1} DQ-collagen (type I from bovine skin conjugated with fluorescein) in 1% gelatin in PBS. Degraded collagen was visualized after fixation and staining for F-actin with phalloidin-Alexa fluor 633.

Immunofluorescence

Cells were cultured on filters at approximately 200,000 cells per filter (only several 1,000 cells adhered) for 1 to 4 hours and fixed for 15 min in 4% PFA in PBS at room temperature. Cells were then permeabilized with 0.1% (v/v) Triton X-100 in PBS for 5 min and blocked with CLSM-buffer (PBS with 20 mM glycine and 3% (w/v) BSA) for 30 min. For immunostaining, the cells were incubated with primary antibodies diluted in CLSM overnight at room temperature. Subsequently, the cells were washed with PBS and incubated with Alexa fluor 488-labeled secondary antibodies and Alexa fluor 546-conjugated phalloidin for 30 min. Finally, cells were washed with PBS prior to embedding in mounting medium containing 0.01% (v/v) Trolox (6-hydroxy-2,5,7,8-tetramethylchroman-2-carboxylic acid) and 68% (v/v) glycerol in 200 mM sodium phosphate buffer at pH 7.5. The cells were imaged with an Olympus FV1000 confocal laser scanning microscope (Olympus, Tokyo, Japan) with a 60× 1.35 NA oil immersion objective.

PIP_2 labeling

Human monocyte derived dendritic cells were grown on filters with 1 μm pores coated with 2.5% gelatin. Cells were disrupted by a brief ultrasound pulse as described (van den Bogaart et al., 2011) with some modifications. In brief, the filters with cells were washed with twice with PBS at room temperature and placed on the bottom of a large glass container with PBS. The tip of the sonicator (Branson Digital Sonifier) was placed 3 cm above the filter and three pulses (10% power, 0.1 s pulse with 1 s interval) were given. Filters were then washed once with buffer containing 20 mM Hepes-KOH, 120 mM K-gluconate, 20 mM K-acetate, 2 mM ATP-Mg and 0.5 mM DTT, pH 7.4, and incubated for 30 min with 1 μM of the

pleckstrin homology domain of phospholipase C delta subunit fused to citrine (PLC -PH) in the same buffer (van den Bogaart et al., 2011). Finally, the filters were washed twice with PBS, fixed with 4% PFA and co-stained with phalloidin-Alexa fluor 546.

Wiskostatin dissolution of podosomes

Dendritic cells were pre-cultured on glass or gelatin-impregnated filters for 1 h followed by incubation for 15, 30, 60, and 120 minutes with 5 μM wiskostatin (40 mM stock in DMSO) and immediate fixation and immunostaining as described above.

OVA and gp120-quantum dot uptake assay

For the conjugation of gp120 to quantum dots, 40 nM biotinylated-gp120 was incubated with 20 nM quantum dots-655 with coupled avidin by mixing for 30 min at 4°C. The coupling was quenched by addition of a 10-fold molar excess of free biotin (to final concentration of 200 nM) (Cambi et al., 2007).

To test the uptake of antigen via protrusive podosome-like structures, dendritic cells were pre-cultured for 2 hours on filters with 1 μm and 400 nm pore sizes that were impregnated with gelatin. Then, the filters were inverted and placed on top of plastic rings filled with culture medium such that the medium contacted the cells on the filter. The opposite (upper) side of the filter was covered with 50 μl of a suspension of 1 nM quantum dots-655 conjugated to gp120. After 30 min incubation, the cells were fixed with 4% PFA and actin was stained with phalloidin-Alexa fluor 488. Cells were imaged by confocal microscopy. To test the uptake of OVA-Alexa fluor 647-labeled antigen we performed the same assay as for gp120-quantum dots, but now we placed 50 μl of a 5 μg ml^{-1} OVA-Alexa fluor 647 on top of the filter.

Several control experiments were performed: (i) competitive inhibition of antigen uptake with 25 μg ml^{-1} mannan, (ii) quantum dots conjugated to biotin instead of gp120, (iii) filters with smaller pore sizes of 400 nm, (iv) CHO cells that stably expressed DC-SIGN (Cambi et al., 2007) instead of dendritic cells and (v) wiskostatin and (vi) Pitstop 2 block of antigen uptake. For the wiskostatin experiment, cells were preincubated for 30 min with 5 μM wiskostatin (40 mM stock in DMSO) and uptake experiments were performed in presence of wiskostatin. For the Pitstop 2 experiment, cells were preincubated for 15 min with 20 μM wiskostatin or Pitstop 2-negative control (both from Abcam; 30 mM stock in DMSO) and uptake experiments were performed in presence of Pitstop 2 or negative control. All experiments were independently repeated at least three times with dendritic cells isolated from different donors and statistical significance (*P*-values) was calculated with 2-tailed student t-test for paired samples.

Passive leakage of antigen through gelatin-coated filters

In order to measure passive diffusion of the quantum dots and OVA through the filters we used either uncoated or gelatin-impregnated filters with pore sizes of 400 nm and 1 μm (prepared as described above). These filters were placed on top of plastic rings filled with PBS. A 50 μl droplet of antigen suspension (0.2 nM for gp120-labeled quantum dots and 5 μg ml^{-1} of OVA-647) was then placed on top of the filter for 30 min. The remaining volume

of antigen suspension (~20 µl) was aspirated from the top of the filter and transferred to the MaxiSorp 96 well plate. The fluorescence intensity was measured with a CytoFluor ll fluorescence well plate reader (PerSeptive Biosystems) (quantum dots-655: excitation: 360/40, emission: 645/40 nm; OVA-Alexa fluor 647: excitation: 590/20, emission: 645/20 nm filters). Each experiment was repeated at least 3 times.

Live cell imaging

Cells were transfected using the Neon Transfection system (Invitrogen) as described (van den Dries et al., 2013a). Briefly, 200,000 cells were washed with PBS and resuspended in 100 µl resuspension buffer R (Invitrogen). These cells were subsequently mixed with 2 µg of a plasmid coding for LifeAct-GFP and electroporated (2 pulses of 40 ms, 1,000 V). Transfected cells were plated in pre-warmed WillCo-dishes (WillCo Wells) containing antibiotic-free and serum-free RPMI medium (Invitrogen). After 3 h of culturing, the medium was replaced by medium supplemented with 10% (v/v) FCS and antibiotics. Prior to live cell imaging, cells were washed with PBS and imaging was performed in RPMI without phenol red supplemented with 10 mM HEPES at pH 7.4. Transiently transfected cells were imaged at 37°C on a Zeiss LSM 510 microscope equipped with a PlanApochromatic 63× 1.4 NA oil immersion objective.

Transmission electron microscopy

For the immuno-gold labeling, dendritic cells were cultured on gelatin-impregnated filters with 1 µm pore size for 1 h, washed once with 0.1 M phosphate buffer at pH 7.4 (PB) and fixed with 2% (w/v) PFA in PB for 2 h. Residual PFA was quenched with 20 mM glycine in PB for 20 min. Samples were blocked with 5% (w/v) BSA-c and 0.1% (w/v) cold water fish gelatin in PB for 20 min. The primary antibody (directed against DC-SIGN or CD206) was incubated overnight at 4°C in 0.1% BSA-c in PB. Secondary rabbit-anti-mouse antibody was incubated for 30 min at 20 µg ml^{-1} and for visualization cells were incubated with 10 nm diameter gold-labeled protein A (binds rabbit IgG) in 0.1% BSA-c in PB. A final fixation step was performed with 2% glutaraldehyde in PB for 60 min at 4°C. Samples were treated for 60 min with 1% (w/v) OsO_4, 1% (w/v) potassium ferrocyanide in 0.1 M sodium cacodylate buffer at pH 7.4. Following dehydration with a graded ethanol series, the filters were embedded in Epon which was left to polymerize for 24 h at 60°C. After polymerization, ~90 nm thin sections perpendicular to the surface of the filter surfaces were cut with a microtome and specimens were imaged with a JEOL 1010 transmission electron microscope.

Transwell inserts with endothelial and epithelial monolayers

Costar Transwell 6.5 mm diameter inserts containing polycarbonate membrane filters with 5 µm pore size (catalogue number 3421; Corning Incorporated) and impregnated with gelatin were cultured with 160,000 cells of the endothelial cell line EA.hy926 in DMEM with 4.5 g l^{-1} glucose, 1 mM ultra-glutamine, antibiotics and 10% FBS on the outer side of the inserts. For the epithelial cell line Caco-2, 5,000 cells were cultured in DMEM with 25 mM glucose, 1% non-essential amino acids, antibiotics and 20% FBS on the outer side of the inserts and without gelatin. Confluent monolayers were formed in 10 days (for EA.hy926) and 20 days (for Caco-2) culturing time. Subsequently, 20,000 to 100,000 dendritic cells were applied to

the inner chamber of the transwell inserts and incubated for 24 hours (for EA.hy926) or 5 hours (for Caco-2). For the uptake experiments of Alexa fluor 647 labeled ovalbumin (OVA647) through the monolayers of Caco-2 cells (Supp. Fig. 1E), 5 μg ml^{-1} OVA-647 in RPMI was added to the outer chamber and incubated for 1 h. Finally the samples were fixed and immunostained for DC-SIGN and CD206 (expressed by dendritic cells).

ELISA and DO11.10 activation assay

For IL-2 production as readout of T-cell activation we used the T-cell hybridoma DO11.10. DO11.10 was grown in IMDM with 5% FCS, 1 mM ultra-glutamine, antibiotics and 0.1% (v/v) β-mercaptoethanol. Immature mouse bone marrow derived dendritic cells (BMDCs) were isolated by culturing for 7 days with GM-CSF (20 ng ml^{-1}). Animal studies were approved by the Animal Ethics Committee of the Nijmegen Animal Experiments Committee. The OVA antigen (concentration used 100 μg ml^{-1}) uptake assay on filters (1 μm pores) was performed as described above for 1 h. The filters were washed 3 times with PBS and DO11.10 cells in RPMI were added to the washed filters and incubated overnight. 200,000 BMDCs and 1×10^6 DO11.10 cells were used, but the ratio of BMDC to T-cells was in the order of 1:20 – 1:200 since only a fraction of the BMDCs adhered to the filter (1,000 – 10,000 cells). After culturing for 6 days IL-2 production was measured by monoclonal capture and HRP-conjugated anti-IL-2 antibodies (554424 and 554426, BD Biosciences) using standard ELISA procedures.

Supplementary Material

Refer to Web version on PubMed Central for supplementary material.

Acknowledgments

We thank Peter Friedl for comments, Jack Fransen for Caco-2 cells and Mietske Wijers for help with the electron microscopy (all Radboud University Medical Centre, The Netherlands). GvdB is funded by a fellowship from the Radboud University Nijmegen Medical Centre and is the recipient of a Starting Grant from the European Research Council under the European Union's Seventh Framework Programme (Grant Agreement Number 336479). AC is the recipient of a grant of the Human Frontier Science Program Organization and of a Meervoud grant from the Netherlands Organization for Scientific Research (NWO). CGF is the recipient of an Advanced Grant from the European Research Council under the European Union's Seventh Framework Programme and of a Spinoza award from NWO.

References

Banchereau J, Steinman RM. Dendritic cells and the control of immunity. Nature. 1998; 392:245–252. [PubMed: 9521319]

Brakebusch C, Fässler R. The integrin-actin connection, an eternal love affair. EMBO J. 2003; 22:2324–2333. [PubMed: 12743027]

Bravo-Cordero JJ, Hodgson L, Condeelis J. Directed cell invasion and migration during metastasis. Curr. Opin. Cell Biol. 2012; 24:277–283. [PubMed: 22209238]

Buccione R, Orth JD, McNiven MA. Foot and mouth: podosomes, invadopodia and circular dorsal ruffles. Nat. Rev. Mol. Cell. Biol. 2004; 5:647–657. [PubMed: 15366708]

Burgdorf S, Lukacs-Kornek V, Kurts C. The mannose receptor mediates uptake of soluble but not of cell-associated antigen for cross-presentation. J. Immunol. 2006; 176:6770–6776. [PubMed: 16709836]

Burns S, Thrasher AJ, Blundell MP, Machesky L, Jones GE. Configuration of human dendritic cell cytoskeleton by Rho GTPases, the WAS protein, and differentiation. Blood. 2001; 98:1142–1149. [PubMed: 11493463]

Calle Y, Carrager NO, Thrasher AJ, Jones GE. Inhibition of calpain stabilises podosomes and impairs dendritic cell motility. J. Cell Sci. 2006; 119:2375–2385. [PubMed: 16723743]

Cambi A, Lidke DS, Arndt-Jovin DJ, Figdor CG, Jovin TM. Ligand-conjugated quantum dots monitor antigen uptake and processing by dendritic cells. Nano Lett. 2007; 7:970–977. [PubMed: 17388641]

Carman CV, Sage PT, Sciuto TE, de la Fuente MA, Geha RS, Ochs HD, Dvorak HF, Dvorak AM, Springer TA. Transcellular diapedesis is initiated by invasive podosomes. Immunity. 2007; 26:784–797. [PubMed: 17570692]

Chieppa M, Rescigno M, Huang AY, Germain RN. Dynamic imaging of dendritic cell extension into the small bowel lumen in response to epithelial cell TLR engagement. J. Exp. Med. 2006; 203:2841–2852. [PubMed: 17145958]

Collin O, Na S, Chowdhury F, Hong M, Shin ME, Wang F, Wang N. Self-organized podosomes are dynamic mechanosensors. Curr. Biol. 2008; 18:1288–1294. [PubMed: 18760605]

Cornfine S, Himmel M, Kopp P, El Azzouzi K, Wiesner C, Krüger M, Rudel T, Linder S. The kinesin KIF9 and reggie/flotillin proteins regulate matrix degradation by macrophage podosomes. Mol. Biol. Cell. 2011; 22:202–215. [PubMed: 21119006]

Cox S, Rosten E, Monypenny J, Jovanovic-Talisman T, Burnette DT, Lippincott-Schwartz J, Jones GE, Heintzmann R. Bayesian localization microscopy reveals nanoscale podosome dynamics. Nat. Methods. 2011; 9:195–200. [PubMed: 22138825]

de Vries IJ, Eggert AA, Scharenborg NM, Vissers JL, Lesterhuis WJ, Boerman OC, Punt CJ, Adema GJ, Figdor CG. Phenotypical and functional characterization of clinical grade dendritic cells. J. Immunother. 2002; 25:429–438. [PubMed: 12218781]

Dovas A, Gevrey JC, Grossi A, Park H, Abou-Kheir W, Cox D. Regulation of podosome dynamics by WASp phosphorylation: implication in matrix degradation and chemotaxis in macrophages. J. Cell Sci. 2009; 122:3873–3882. [PubMed: 19808890]

Dutta D, Williamson CD, Cole NB, Donaldson JG. Pitstop 2 is a potent inhibitor of clathrin-independent endocytosis. PLoS One. 2012; 7:e45799. [PubMed: 23029248]

Farache J, Koren I, Milo I, Gurevich I, Kim KW, Zigmond E, Furtado GC, Lira SA, Shakhar G. Luminal bacteria recruit CD103+ dendritic cells into the intestinal epithelium to sample bacterial antigens for presentation. Immunity. 2013; 38:581–595. [PubMed: 23395676]

Gawden-Bone C, Zhou Z, King E, Prescott A, Watts C, Lucocq J. Dendritic cell podosomes are protrusive and invade the extracellular matrix using metalloproteinase MMP-14. J. Cell Sci. 2010; 123:1427–1437. [PubMed: 20356925]

Geijtenbeek TB, Kwon DS, Torensma R, van Vliet SJ, van Duijnhoven GC, Middel J, Cornelissen IL, Nottet HS, KewalRamani VN, Littman DR, et al. DC-SIGN, a dendritic cell-specific HIV-1-binding protein that enhances trans-infection of T cells. Cell. 2000; 100:587–597. [PubMed: 10721995]

Gimona M, Buccione R, Courtneidge SA, Linder S. Assembly and biological role of podosomes and invadopodia. Curr. Opin. Cell Biol. 2008; 20:235–241. [PubMed: 18337078]

Jones GE, Zicha D, Dunn GA, Blundell M, Thrasher A. Restoration of podosomes and chemotaxis in Wiskott-Aldrych syndrome macrophages following expression of WASp. Int. J. Biochem. Cell Biol. 2002; 34:806–815. [PubMed: 11950596]

Kaparakis M, Philpott DJ, Ferrero RL. Mammalian NLR proteins; discriminating foe from friend. Immunol. Cell Biol. 2007; 85:495–502. [PubMed: 17680011]

Labernadie A, Thibault C, Vieu C, Maridonneau-Parini I, Charrière GM. Dynamics of podosome stiffness revealed by atomic force microscopy. Proc. Natl. Acad. Sci. USA. 2010; 107:21016–21021. [PubMed: 21081699]

Lelouard H, Fallet M, de Bovis B, Méresse S, Gorvel JP. Peyer's patch dendritic cells sample antigens by extending dendrites through M cell-specific transcellular pores. Gastroenterology. 2012; 142:592–601. [PubMed: 22155637]

Linder S. The matrix corroded: podosomes and invadopodia in extracellular matrix degradation. Trends Cell Biol. 2007; 17:107–117. [PubMed: 17275303]

Linder S, Nelson D, Weiss M, Aepfelbacher M. Wiskott-Aldrich syndrome protein regulates podosomes in primary human macrophages. Proc. Natl. Acad. Sci. USA. 1999; 96:9648–9653. [PubMed: 10449748]

Linder S, Wiesner C, Himmal M. Degrading devices: invadosomes in proteolytic cell invasion. Annu. Rev. Cell. Dev. Biol. 2011; 27:185–211. [PubMed: 21801014]

Lipscomb MF, Masten BJ. Dendritic cells: immune regulators in health and disease. Physiol. Rev. 2002; 82:97–130. [PubMed: 11773610]

Matías-Román S, Gálvez BG, Genís L, Yáñez-Mó M, de la Rosa G, Sánchez-Mateos P, Sánchez-Madrid F, Arroyo AG. Membrane type 1-matrix metalloproteinase is involved in migration of human monocytes and is regulated through their interaction with fibronectin or endothelium. Blood. 2005; 105:3956–3964. [PubMed: 15665118]

McGreal EP, Miller JL, Gordon S. Ligand recognition by antigen-presenting cell C-type lectin receptors. Curr. Opin. Immunol. 2005; 17:18–24. [PubMed: 15653305]

Muller WA. Mechanisms of leukocyte transendothelial migration. Annu. Rev. Pathol. 2011; 6:323–344. [PubMed: 21073340]

Murphy DA, Courtneidge SA. The ‘ins’ and ‘outs’ of podosomes and invadopodia: characteristics, formation and function. Nat. Rev. Mol. Cell Biol. 2011; 12:413–426. [PubMed: 21697900]

Niess JH, Brand S, Gu X, Landsman L, Jung S, McCormick BA, Vyas JM, Boes M, Ploegh HL, Fox JG, et al. CX3CR1-mediated dendritic cell access to the intestinal lumen and bacterial clearance. Science. 2005; 307:254–258. [PubMed: 15653504]

Peterson JR, Bickford LC, Morgan D, Kim AS, Ouerfelli O, Kirschner MW, Rosen MK. Chemical inhibition of N-WASP by stabilization of a native autoinhibited conformation. Nat. Struct. Mol. Biol. 2004; 11:747–755. [PubMed: 15235593]

Prehoda KE, Scott JA, Mullins RD, Lim WA. Integration of multiple signals through cooperative regulation of the N-WASP-Arp2/3 complex. Science. 2000; 290:801–806. [PubMed: 11052943]

Proszynski TJ, Gingras J, Valdez G, Krzewski K, Sanes JR. Podosomes are present in a postsynaptic apparatus and participate in its maturation. Proc. Natl. Acad. Sci. USA. 2009; 106:18373–18378. [PubMed: 19822767]

Quaranta V, Walker LE, Pellegrino MA, Ferrone S. Purification of immunologically functional subsets of human Ia-like antigens on a monoclonal antibody (Q5/13) immunoadsorbent. J. Immunol. 1980; 125:1421–1425. [PubMed: 6157732]

Rescigno M, Urbano M, Valzasina B, Francolini M, Rotta G, Bonasio R, Granucci F, Kraehenbuhl JP, Ricciardi-Castagnoli P. Dendritic cells express tight junction proteins and penetrate gut epithelial monolayers to sample bacteria. Nat. Immunol. 2001; 2:361–367. [PubMed: 11276208]

Sabeh F, Ota I, Holmbeck K, Birkedal-Hansen H, Soloway P, Balbin M, Lopez-Otin C, Shapiro S, Inada M, Krane S, et al. Tumor cell traffic through the extracellular matrix is controlled by the membrane-anchored collagenase MT1-MMP. J. Cell Biol. 2004; 167:769–781. [PubMed: 15557125]

Sage PT, Varghese LM, Martinelli R, Sciuto TE, Kamei M, Dvorak AM, Springer TA, Sharpe AH, Carman CV. Antigen recognition is facilitated by invadosome-like protrusions formed by memory/effector T cells. J. Immunol. 2012; 188:3686–3699. [PubMed: 22442443]

Schachtner H, Calaminus SD, Sinclair A, Monypenny J, Blundell MP, Leon C, Holyoake TL, Thrasher AJ, Michie AM, Vukovic M, et al. Megakaryocytes assemble podosomes that degrade matrix and protrude through basement membrane. Blood. 2013a; 121:2542–2552. [PubMed: 23305739]

Schachtner H, Calaminus SD, Thomas SG, Machesky LM. Podosomes in adhesion, migration, mechanosensing and matrix remodeling. Cytoskeleton (Hoboken). 2013b; 70:572–589. [PubMed: 23804547]

Schmidt S, Nakchbandi I, Ruppert R, Kawelke N, Hess MW, Pfaller K, Jurdic P, Fässler R, Moser M. Kindlin-3-mediated signaling from multiple integrin classes is required for osteoclast-mediated bone resorption. J. Cell Biol. 2011; 192:883–897. [PubMed: 21357746]

Schoumacher M, Goldman RD, Louvard D, Vignjevic DM. Actin, microtubules, and vimentin intermediate filaments cooperate for elongation of invadopodia. J. Cell Biol. 2010; 189:541–556. [PubMed: 20421424]

Shan M, Gentile M, Yeiser JR, Walland AC, Bornstein VU, Chen K, He B, Cassis L, Bigas A, Cols M, et al. Mucus enhances gut homeostasis and oral tolerance by delivering immunoregulatory signals. Science. 2013; 342:447–453. [PubMed: 24072822]

Shimonkevitz R, Kappler J, Marrack P, Grey H. Antigen recognition by H-2-restricted T cells. I. Cell-free antigen processing. J. Exp. Med. 1983; 158:303–316. [PubMed: 6193218]

Strisciuglio C, Duijvestein M, Verhaar AP, Vos AC, van den Brink GR, Hommes DW, Wildenberg ME. Impaired autophagy leads to abnormal dendritic cell-epithelial cell interactions. J. Crohns Colitis. 2013; 7:534–541. [PubMed: 22981596]

Takeda K, Akira S. Toll-like receptors in innate immunity. Int. Immunol. 2005; 17:1–14. [PubMed: 15585605]

Thornton EE, Looney MR, Bose O, Sen D, Sheppard D, Locksley R, Huang X, Krummel MF. Spatiotemporally separated antigen uptake by alveolar dendritic cells and airway presentation to T cells in the lung. J. Exp. Med. 2012; 209:1183–1199. [PubMed: 22585735]

Tsujita K, Kondo A, Kurisu S, Hasegawa J, Itoh T, Takenawa T. Antagonistic regulation of F-BAR protein assemblies controls actin polymerization during podosome formation. J. Cell Sci. 2013; 126:2267–2278. [PubMed: 23525018]

Vallon-Eberhard A, Landsman L, Yogev N, Verrier B, Jung S. Transepithelial pathogen uptake into the small intestinal lamina propria. J. Immunol. 2006; 176:2465–2469. [PubMed: 16456006]

van den Bogaart G, Meyenberg K, Risselada HJ, Amin H, Willig KI, Hubrich BE, Dier M, Hell SW, Grubmüller H, Diederichsen U, Jahn R. Membrane protein sequestering by ionic protein-lipid interactions. Nature. 2011; 479:552–555. [PubMed: 22020284]

van den Dries K, van Helden SF, te Riet J, Diez-Ahedo R, Manzo C, Oud MM, van Leeuwen FN, Brock R, Garcia-Parajo MF, Cambi A, Figdor CG. Geometry sensing by dendritic cells dictates spatial organization and PGE(2)-induced dissolution of podosomes. Cell. Mol. Life Sci. 2012; 69:1889–1901. [PubMed: 22204022]

van den Dries K, Meddens MB, de Keijzer S, Shekhar S, Subramaniam V, Figdor CG, Cambi A. Interplay between myosin IIA-mediated contractility and actin network integrity orchestrates podosome composition and oscillations. Nat. Commun. 2013a; 4:1412. [PubMed: 23361003]

van den Dries K, Schwartz SL, Byars J, Meddens MB, Bolomini-Vittori M, Lidke DS, Figdor CG, Lidke KA, Cambi A. Dual color super-resolution microscopy reveals nanoscale organization of mechanosensory podosomes. Mol. Biol. Cell. 2013b; 24:2112–2123. [PubMed: 23637461]

van Helden SF, Krooshoop DJ, Broers KC, Raymakers RA, Figdor CG, van Leeuwen FN. A critical role for prostaglandin E2 in podosome dissolution and induction of high-speed migration during dendritic cell maturation. J. Immunol. 2006; 177:1567–1574. [PubMed: 16849464]

Vestweber D. Novel insights into leukocyte extravasation. Curr. Opin. Hematol. 2012; 19:212–217. [PubMed: 22395664]

von Kleist L, Stahlschmidt W, Bulut H, Gromova K, Puchkov D, Robertson MJ, MacGregor KA, Tomilin N, Pechstein A, Chau N, et al. Role of the clathrin terminal domain in regulating coated pit dynamics revealed by small molecule inhibition. Cell. 2011; 146:471–484. [PubMed: 21816279]

West MA, Prescott AR, Chan KM, Zhou Z, Rose-John S, Scheller J, Watts C. TLR ligand-induced podosome disassembly in dendritic cells is ADAM17 dependent. J. Cell Biol. 2008; 182:993–1005. [PubMed: 18762577]

Wiesner C, Faix J, Himmel M, Bentzien F, Linder S. KIF5B and KIF3A/KIF3B kinesins drive MT1-MMP surface exposure, CD44 shedding, and extracellular matrix degradation in primary macrophages. Blood. 2010; 116:1559–1569. [PubMed: 20505159]

Wolf K, Friedl P. Mapping proteolytic cancer cell-extracellular matrix interfaces. Clin. Exp. Metastasis. 2009; 26:289–298. [PubMed: 18600304]

Wolf K, Te Lindert M, Krause M, Alexander S, Te Riet J, Willis AL, Hoffman RM, Figdor CG, Weiss SJ, Friedl P. Physical limits of cell migration: Control by ECM space and nuclear deformation and tuning by proteolysis and traction force. J. Cell Biol. 2013; 201:1069–1084. [PubMed: 23798731]

Yamaguchi H, Yoshida S, Muroi E, Kawamura M, Kouchi Z, Nakamura Y, Sakai R, Fukami K. Phosphatidylinositol 4,5-bisphosphate and PIP5-kinase Ialpha are required for invadopodia formation in human breast cancer cells. Cancer Sci. 2010; 101:1632–1638. [PubMed: 20426790]

Zicha D, Allen WE, Brickell PM, Kinnon C, Dunn GA, Jones GE, Thrasher AJ. Chemotaxis of macrophages is abolished in the Wiskott-Aldrich syndrome. Br. J. Haematol. 1998; 101:659–665. [PubMed: 9674738]

Europe PMC Funders Author Manuscripts

Europe PMC Funders Author Manuscripts

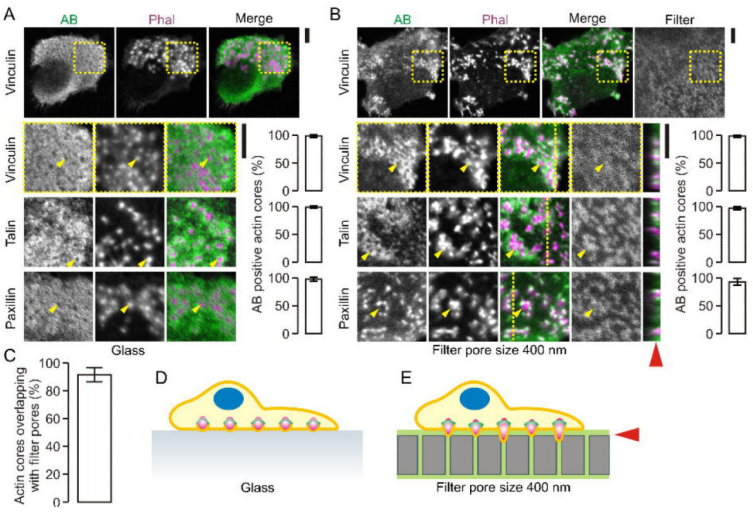

Figure 1. Podosomes locate to spots of low physical resistance of the substrate

(A) Human monocyte derived dendritic cells cultured on glass substrate and stained with primary antibodies directed against vinculin, talin and paxillin and secondary antibodies conjugated to Alexa fluor 488 (AB; green). Actin was stained with phalloidin-Alexa fluor 564 (Phal; magenta). Shown are confocal images immediately at the glass surface of representative cells with podosomes. Yellow arrow heads indicate randomly chosen podosomes. Bar graphs show quantification of AB positive actin cores (± SD). (B) Same as panel A, but now for cells on polycarbonate filters with pore sizes of 400 nm. The filters were soaked in gelatin conjugated to Alexa fluor 633 (Filter; grey). Yellow lines indicate the positions of the orthogonal views. The red arrow head indicates the approximate filter surface. (C) Quantification of the alignment of the podosomes to the filter pores from panel B (± SD). (D–E) Schemes of dendritic cells with non-protrusive podosome on glass (D) and filters with pore sizes of 400 nm (E) (actin: magenta; vinculin: green). Scale bars, 5 μm.

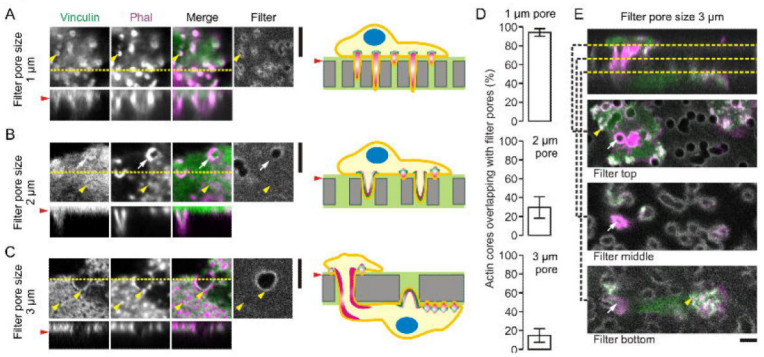

Figure 2. Podosome-like protrusive structures of dendritic cells

(A) Dendritic cells cultured on polycarbonate membrane filters impregnated with Alexa fluor 633-labeled gelatin (grey) with pore sizes of 1 μm. Cells were immunostained for vinculin (green) and actin was visualized by phalloidin (Phal; magenta) similar to figure 1. Shown are confocal sections just above the surface of the filters. The yellow line indicates the position of the orthogonal views showing the protrusion of actin in the lumen of the pores. Yellow arrow heads depict randomly selected actin-rich cores. The red arrow head indicates the approximate filter surface. The right hand panel shows a schematic diagram of the protrusions (actin: magenta; vinculin: green). (B) Same as panel A, but now for filters with pore sizes of 2 μm and showing the protrusion of both the actin core and vinculin in the pores as indicated by the white arrows. The cells also formed podosomes that did not overlap with the pores as indicated by the yellow arrow heads. (C) Same as panel B, but now with pore sizes of 3 μm. (D) Quantification of the fraction of actin cores aligning with the filter pores from panels A–C (± SD). (E) Same as panel C, showing cell migration through the 3 μm pores in the filter (white arrows) and the formation of podosomes on both sides of the filter (yellow arrow heads). Confocal sections above, through and underneath the filter are shown. Scale bars, 5 μm.

Europe PMC Funders Author Manuscripts

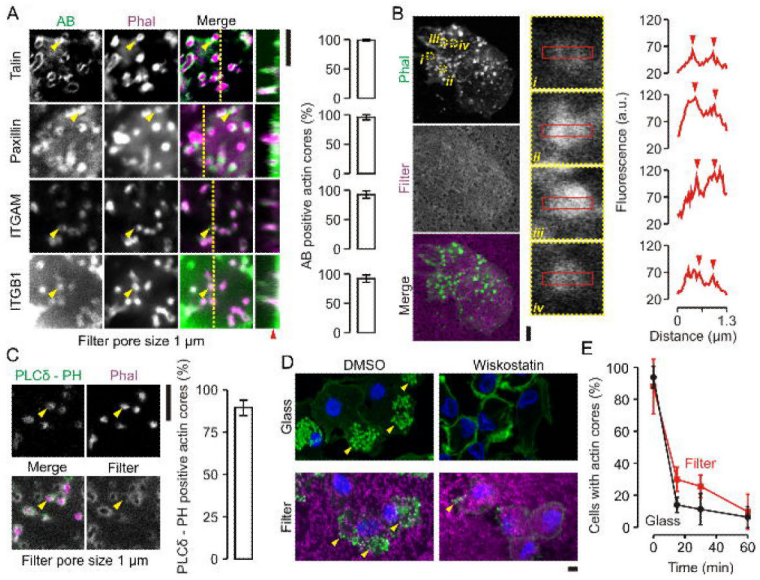

Figure 3. Characterization of protrusive podosome-like structures

(A) Confocal images of human dendritic cells cultured on membrane filters with pore sizes of 1 µm. Actin was stained with phalloidin-Alexa fluor 546 (Phal; magenta) and talin, paxillin, ITGAM and ITGB1 were labeled by specific monoclonal antibodies and secondary antibodies conjugated to Alexa fluor 488 (AB; green). Yellow lines indicate the positions of the orthogonal views. Yellow arrow heads indicate randomly chosen actin cores. Red arrow head indicates the approximate surfaces of the filter substrates. Bar-graphs show quantifications of the fractions of AB positive actin cores (± SD). (B) Confocal image of a dendritic cell on gelatin-Alexa fluor 633 impregnated filters with pore sizes of 1 µm (Filter; magenta) and stained with phalloidin-Alexa fluor 488 (green). The insets show magnifications of actin cores marked *i*–*iv*. The graphs show fluorescence intensity distributions through the cross-sections marked by the red boxes (*y*-averaging). The orange arrow heads mark intensity peaks at the edges of ring structures of some of the actin cores. (C) Same as panel A, but instead of antibody staining, PIP_2 was labeled with bacterially expressed pleckstrin homology domain of phospholipase C delta subunit fused to citrine (PLC -PH). (D) Cells precultured for 1 h on glass or gelatin-Alexa fluor 633 impregnated filters with pore sizes of 1 µm (magenta) were treated for 1 hr with 5 µM of the WASP inhibitor wiskostatin or with carrier only (DMSO). Yellow arrow heads mark clusters of actin cores stained by phalloidin-Alexa fluor 488 (green). (E) The fractions of cells containing actin cores from panel D on glass (black) and filter (red) as a function of exposure time to wiskostatin (± SD, 3 independent repeats). Scale bars, 5 µm.

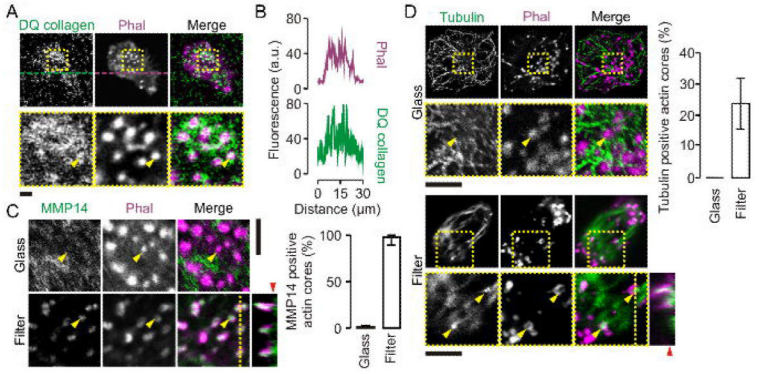

Figure 4. Podosome-like protrusive structures contain MMP14 and tubulin

(A) Confocal images of dendritic cells cultured on filters with 1 µm pore sizes that were impregnated with double-quenched FITC-labeled collagen in gelatin (DQ collagen; green). Actin was stained with phalloidin-Alexa fluor 633 (Phal; magenta). Collagen degradation results in loss of self-quenching of the FITC fluorophore and an increase in fluorescence. (B) Fluorescence intensity profiles from panel A marked by the dashed lines. (C) Confocal images (left) and quantification (right) of dendritic cells cultured on glass and membrane filters with pore sizes of 1 µm. Actin was stained with phalloidin-Alexa fluor 546 (magenta) and the metalloprotease MMP-14 was labeled by specific monoclonal antibodies and secondary antibodies conjugated to Alexa fluor 488 (AB; green). The yellow line indicates the positions of the orthogonal view. The yellow arrow heads indicate randomly chosen actin cores. The red arrow head indicates the approximate surface of the filter. (D) Same as panel C, but now for tubulin. Error bars show the spread of data for multiple cells from at least two independent experiments. Scale bars, 5 µm.

Europe PMC Funders Author Manuscripts

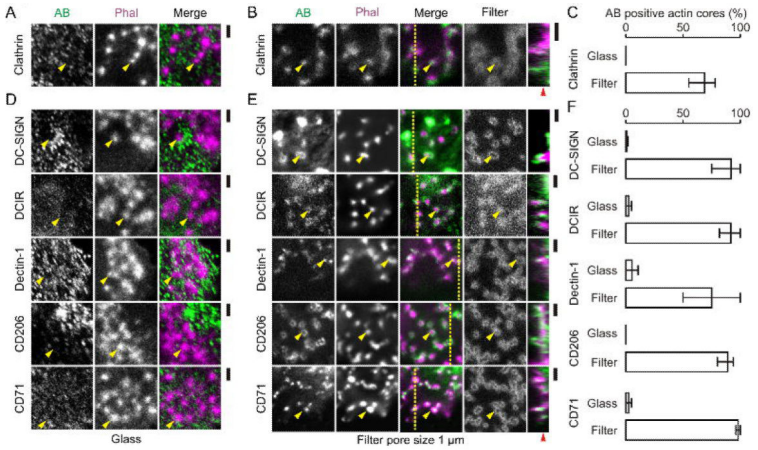

Figure 5. Protrusive podosome-like structures contain pattern recognition receptors

(A–B) Confocal images of dendritic cells cultured on glass (A) and on filters with 1 µm pore size (B). Actin was labeled with phalloidin-Alexa fluor 546 (Phal; magenta) and clathrin was visualized by immunostaining (AB; green). The filters were impregnated with Alexa fluor 633-labeled gelatin (Filter; grey). The yellow line indicates the position of the orthogonal view. Yellow arrow heads indicate randomly selected actin-rich cores. The red arrow head indicates the approximate filter surface. (C) Quantification of the fraction of clathrin positive actin cores from panels A–B. (D–F) Same as panels A–C, but now with immunostaining for DC-SIGN, DCIR, Dectin-1, CD206 and CD71. Error bars show the spread of data for multiple cells from at least two independent experiments. Scale bars, 2 µm.

Europe PMC Funders Author Manuscripts

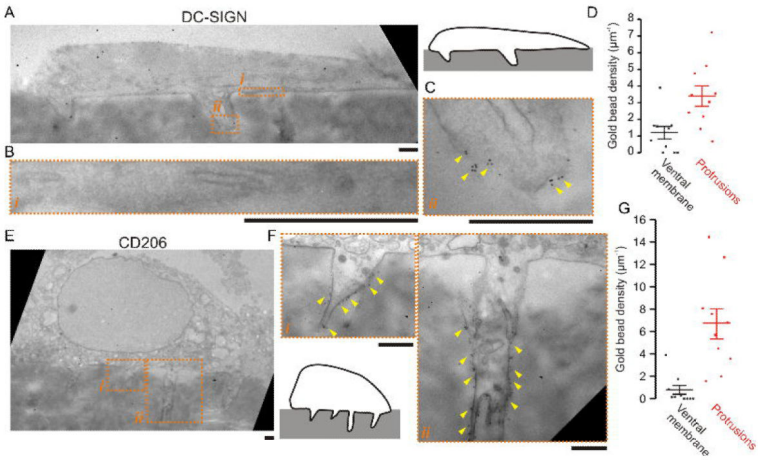

Figure 6. Transmission electron microscopy of protrusive podosome-like structures

(A) Electron micrographs of a human dendritic cell cultured on gelatin impregnated filters with 1 µm pore size and immuno-gold labeled for DC-SIGN (inset, overview). (B–C) Details of the ventral membrane (B, marked *i* in panel A) and of a protrusive structure (C, *ii*) from panel A. Yellow arrow heads mark positions of clusters of gold beads. (D) Quantification of the gold beads per µm imaged membrane for 10 different cells at the ventral membrane (black) and the protrusions (red). Data points for individual cells and the average are shown (± SEM). Bead density was 3-fold increased at the protrusions relative to ventral membrane ($P = 0.0005$, 2-tailed paired t-test). (E) Same as panel A, but now with immuno-gold labeling for CD206. (F) Magnifications of panel E as indicated (*i*, *ii*). (G) Same as panel D, but now for CD206. Bead density was 9-fold increased at the protrusions relative to ventral membrane ($P = 0.002$, 2-tailed paired t-test). Scale bars, 1 µm.

Europe PMC Funders Author Manuscripts

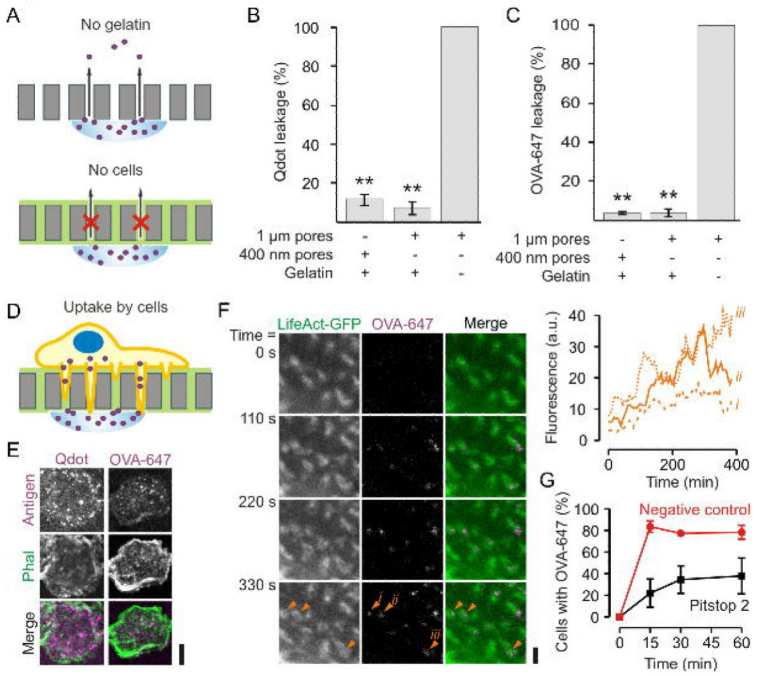

Figure 7. Antigen uptake by protrusive podosome-like structures

(A) Schematics of the control experiments for passive leakage of quantum dots or OVA-Alexa fluor 647 (OVA-647) through the filters. (B–C) Leakage assay of quantum dots (B) or OVA-647 (C) through filters with different pore sizes and with or without gelatin impregnation. (D) Scheme of the antigen uptake experiments. (E) Confocal images of dendritic cells cultured on gelatin-coated filters with 1 µm pore sizes. A suspension of quantum dots linked to gp120 (Qdot; left; magenta) or a solution of OVA-647 (right; magenta) was applied to the other side of the filter. The cells were stained with phalloidin-Alexa fluor 488 (Phal; green) and imaged after 1 hr incubation (see Fig. 8A–B for quantification). (F) Live cell imaging of dendritic cells tranfected with LifeAct-GFP and cultured on filter. At time $t = 0$, OVA-647 was applied to the other side of the filter. The inset shows the increase of OVA-647 fluorescence in time at the position of 3 actin cores marked with orange arrow heads (*i – iii*). Full dataset is in Supplementary Movie 3. (G) Time course of OVA-647 uptake for dendritic cells on filter treated with 20 µM Pitstop 2 (red) or Pitstop 2-negative control (black) (± SEM of three independent repeats). Scale bars: E, 10 µm; F: 2 µm.

Europe PMC Funders Author Manuscripts

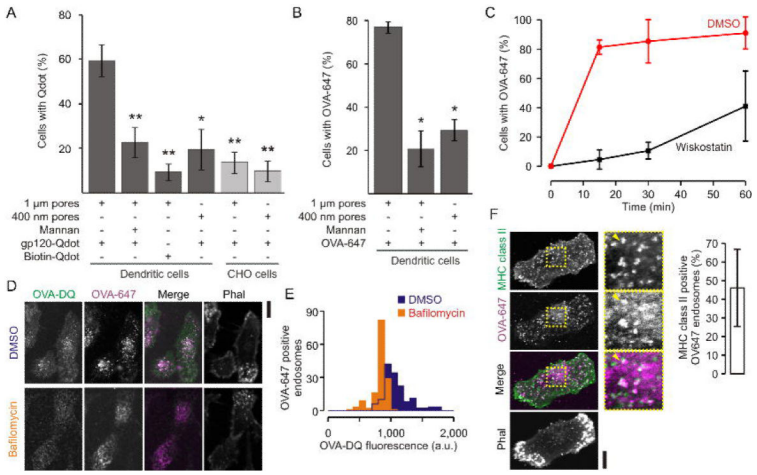

Figure 8. Antigen uptake and processing by protrusive podosome-like structures

(A) Uptake assay as described in figure 7 for human dendritic cells and CHO cells stably expressing DC-SIGN cultured on gelatin-coated filters with 1 µm or 400 nm pore sizes and in the presence or absence of 25 µg ml^{-1} mannan. After 1 h uptake, the fraction of cells that took up gp120 or biotin labeled quantum dots (gp120-Qdot; Biotin-Qdot) was determined by analysis of confocal images by 2 or 3 independent experts (> 3 independent repeats; ± SEM; *, $P < 0.02$; **, $P << 0.01$). (B) Same as panel A, but now for OVA-647. (C) Time course of OVA-647 uptake for dendritic cells on filter treated with 5 µM wiskostatin (black) or carrier only (DMSO; red) (± SEM of three independent repeats). (D) Confocal images of dendritic cells cultured on gelatin-coated filters with 1 µm pore sizes and with uptake of double quenched OVA (OVA-DQ; green) and OVA-Alexa fluor 647 (OVA-647; magenta) through the filter. Actin was stained with phalloidin-Alexa fluor 564 (Phal; grey). OVA-DQ was dequenched as apparent from the increased fluorescence compared to cells treated with bafilomycin A1 (control). (E) Distribution of the OVA-DQ fluorescence of OVA-647 positive compartments for the bafilomycin treated and control cells from panel A (at least 5 cells each). (F) Uptake of OVA-647 (magenta) by dendritic cells on filter and immunostained for MHC class II (green). Actin was stained with phalloidin-Alexa fluor 546 (Phal; grey). Yellow arrow heads indicate MHC class II compartments. Bar-graphs show quantifications of MHC class II positive OVA-647 compartments (± SD). Scale bars, 10 µm.

Europe PMC Funders Author Manuscripts